

Epigenetic downregulation of TET3 reduces genome-wide 5hmC levels and promotes glioblastoma tumorigenesis

Antonella Carella^{1*}, Juan R. Tejedor^{1,2*}, María G. García¹, Rocío G. Urdinguio³, Gustavo F. Bayón¹, Marta Sierra¹, Virginia López³, Estela García-Toraño¹, Pablo Santamarina-Ojeda^{1,2}, Raúl F. Pérez³, Timothée Bigot^{1,2}, Cristina Mangas¹, María D. Corte-Torres⁴, Inés Sáenz-de-Santa-María⁵, Manuela Mollejo⁶, Bárbara Meléndez⁶, Aurora Astudillo⁷, María D. Chiara  Agustín F. Fernández^{1,2} and Mario F. Fraga 

¹Instituto Universitario de Oncología del Principado de Asturias (IUOPA), Hospital Universitario Central de Asturias (HUCA), Universidad de Oviedo, Oviedo, Spain

²Fundación para la Investigación Biosanitaria de Asturias (FINBA), Instituto de Investigación Sanitaria del Principado de Asturias (ISPA), Oviedo, Spain

³Nanomaterials and Nanotechnology Research Center (CINN-CSIC), Universidad de Oviedo, Oviedo, Spain

⁴Hospital Universitario Central de Asturias (HUCA), Biobanco del Principado de Asturias, Oviedo, Spain

⁵Hospital Universitario Central de Asturias (HUCA), Servicio de Otorrinolaringología, Instituto Universitario de Oncología del Principado de Asturias (IUOPA), Universidad de Oviedo, CIBERONC, Oviedo, Spain

⁶Departamento de Patología, Hospital Virgen de la Salud (CHT), Toledo, Spain

⁷Departamento de Anatomía Patológica, Hospital Universitario Central de Asturias (HUCA), Oviedo, Spain

Loss of 5-hydroxymethylcytosine (5hmC) has been associated with mutations of the ten–eleven translocation (TET) enzymes in several types of cancer. However, tumors with wild-type *TET* genes can also display low 5hmC levels, suggesting that other mechanisms involved in gene regulation might be implicated in the decline of this epigenetic mark. Here we show that DNA hypermethylation and loss of DNA hydroxymethylation, as well as a marked reduction of activating histone marks in the *TET3* gene, impair *TET3* expression and lead to a genome-wide reduction in 5hmC levels in glioma samples and cancer cell lines. Epigenetic drugs increased expression of *TET3* in glioblastoma cells and ectopic overexpression of *TET3* impaired *in vitro* cell growth and markedly reduced tumor formation in immunodeficient mice models. *TET3* overexpression partially restored the genome-wide patterns of 5hmC characteristic of control brain samples in glioblastoma cell lines, while elevated *TET3* mRNA levels were correlated with better prognosis in glioma samples. Our results suggest that epigenetic repression of *TET3* might promote glioblastoma tumorigenesis through the genome-wide alteration of 5hmC.

Key words: DNA methylation, 5-hydroxymethylcytosine, *TET3*, glioma, methylation arrays

Abbreviations: 5hmC: 5-hydroxymethylcytosine; 5mC: 5-methylcytosine; ChIP: chromatin immunoprecipitation; dhmCpGs: differentially hydroxymethylated CpGs; DMEM: Dulbecco modified Eagle medium; ENCODE: encyclopedia of DNA elements; GBM: glioblastoma multiforme; GLM: general linear model; GO: gene ontology; GTEx: genotype-tissue expression; KEGG: Kyoto Encyclopedia of Genes and Genomes; MTT: 3-(4,5-dimethylthiazol-2-yl)-2,5-diphenyltetrazolium bromide; OR: odd ratio; PCR: polymerase chain reaction; RTCA: real-time cell analysis system; RT-qPCR: quantitative reverse transcription PCR; SAHA: suberoylanilide hydroxamic acid; TET: ten–eleven translocation; WGBS: whole genome bisulfite sequencing

Additional Supporting Information may be found in the online version of this article.

Conflict of interest: None declared.

Grant sponsor: FICYT; **Grant sponsor:** FINBA / ISPA; **Grant sponsor:** Fundación Científica Asociación Española Contra el Cáncer;

Grant sponsor: Fundación Ramón Areces; **Grant sponsor:** Gobierno del Principado de Asturias (ES) / FEDER;

Grant number: GRUPIN14-052; **Grant sponsor:** ISCIII Subdirección General de Evaluación y Fomento de la Investigación;

Grant number: CP11/00131; **Grant sponsor:** IUOPA; **Grant sponsor:** Ministerio de Economía, Industria y Competitividad, Gobierno de España; **Grant numbers:** FJCI-2015-26965, IJCI-2015-23316, RTC-2015-3393-1; **Grant sponsor:** Plan Nacional de I+D+I 2013/2016 FEDER; **Grant number:** PI15/00892

*A.C. and J.R.T. contributed equally to this work

DOI: 10.1002/ijc.32520

History: Received 12 Dec 2018; Accepted 4 Jun 2019; Online 18 Jun 2019

Correspondence to: Mario F. Fraga, Avenida de Roma s/n, 33011 Oviedo, Asturias, Spain, Tel.: +34-985733644, E-mail: mffraga@cinn.es; or Agustín F. Fernández, Avenida de Roma s/n, 33011 Oviedo, Asturias, Spain, Tel.: +34-985652411, E-mail: afernandez@hca.es

What's new?

Reduced levels of 5-hydroxymethylcytosine (5hmC), an epigenetic mark generated by TET enzymes, have been observed in multiple cancers. Although mutations in TET enzymes have been associated with 5hmC loss, other mechanisms may be at play. Here, the authors show that DNA hypermethylation, loss of DNA hydroxymethylation, and reduction of activating histone marks in the TET3 gene impair TET3 expression and lead to a genome-wide reduction in 5hmC levels in glioma. Important protease inhibitor and TET3 downstream target gene RECK might help mediate tumorigenesis. The results suggest that epigenetic repression of TET3 promotes glioblastoma tumorigenesis through the genome-wide alteration of 5hmC.

Introduction

DNA methylation is a critical epigenetic modification and is strongly associated with the regulation of gene transcription.¹ 5-Methylcytosine (5mC) plays a crucial role in cellular development² and has been implicated in numerous pathological states including cancer.^{3,4} As such, the discovery of a new cytosine modification in mammalian genomes, 5-hydroxymethylcytosine (5hmC), was also a notable breakthrough to the epigenetic research field.⁵ 5hmC is generated by ten-eleven translocation (TET) enzymes (TET1, TET2 and TET3), a family of α -ketoglutarate and Fe-dependent dioxygenases which share a high degree of homology within their C-terminal catalytic domain.⁶

The study of 5hmC has rapidly intensified and recent results have shown that TET proteins and 5hmC are involved in gene regulation and development.^{7,8} These studies revealed that 5hmC is enriched in gene promoters, distal enhancer regulatory regions and gene bodies,⁹ suggesting that 5hmC is not only a merely intermediate of DNA demethylation but acts as a stable epigenetic mark, directly influencing chromatin structure and genome function.

The levels of 5hmC are approximately 10-fold more abundant in brain than in other tissues, suggesting that 5hmC might have a potential function within the nervous system as an important epigenetic marker.¹⁰ Furthermore, it is well established that levels of 5hmC in cancer are severely impaired as compared to those in the corresponding normal tissue. This loss of 5hmC has been reported in multiple human cancers, such as melanoma, breast, colon, glioblastoma multiforme (GBM) and liver,^{11–14} and is closely related to the onset and development of tumors, suggesting that it might be an important marker for the early diagnosis of cancer.

Depending on tumor type, loss of 5hmC might be induced by different mechanisms. This phenomenon may be associated with mutations in the isocitrate dehydrogenase genes *IDH1/2*, with a consequent depletion of the essential TET cosubstrate α -ketoglutarate, or mutations of TET enzymes.^{15–17} Interestingly, deficiency of L-ascorbic acid—a reducing agent that promotes the recycling of TET cofactor Fe^{2+} —or enhanced replication-dependent processes—as a result of the increased proliferation of tumor cells—do not allow the complete reestablishment of 5hmC levels by TET family enzymes.^{18–20} Indeed, some studies have reported that tumors with wild-type *TET* or wild-type *IDH* genes can also present a notable loss of 5hmC levels.^{21,22} Hence the biological significance and molecular mechanisms of 5hmC impairment in human cancer still need to be addressed.

Recent work has demonstrated a critical role for TET3 in the process of neural differentiation,²³ and disruption of TET3 levels has been associated with glioblastoma stem cell self-renewal and tumorigenesis.²⁴ Thus, in our study, we explored potential sources of TET3 epigenetic downregulation in glioblastoma, and the subsequent consequences on overall 5hmC levels in brain tumors. We found that DNA hypermethylation and loss of DNA hydroxymethylation, as well as a reduction in activating histone marks, in the genomic context of *TET3* impairs TET3 expression and leads to a genome-wide reduction of 5hmC levels in glioblastoma samples. Restoration of TET3 expression in glioblastoma cell lines partially recapitulated the pattern of 5hmC observed in healthy human brain and clearly diminished the proliferative potential of tumor cells. We also identified a subset of downstream target genes regulated by TET3 activity, including important protease inhibitors such as *RECK*, that might mediate the tumorigenic potential of gliomas upon reduction of 5hmC levels. These results may help to elucidate the functional consequences of reduced 5hmC levels in glioblastoma samples mediated by the epigenetic silencing of *TET3*.

Materials and Methods**Acquisition of human brain and glioma samples**

Control brains ($n = 5$) and tumor samples ($n = 9$) were collected from the Hospital Universitario Central de Asturias (HUCA). A second cohort of samples including healthy brain biopsies ($n = 12$ of paired gray and white matter) and tumor samples ($n = 12$) was obtained from the Banc the Teixits Neurològics-Biobanc Hospital Clinic-IDIBAPS (Barcelona) and the Hospital Virgen de la Salud (Toledo), respectively. Informed consent was obtained from all patients involved in our study. The study conducted was approved by the Clinical Research Ethics Committee of the Principality of Asturias. Information regarding the clinical and pathological status of the samples used, including the presence of *IDH1* mutations, is provided in Supporting Information Table S1.

Culture of human cancer cell lines and drug treatments

Human glioblastoma cell line LN229 was cultured according to American Type Culture Collection (ATCC) recommendations. LN229 cells were authenticated using short tandem repeat profiling AmpFLSTR™ Identifier™ Plus PCR Amplification Kit for high-resolution screening and interspecies cross-contamination detection. Cells were grown in Dulbecco-modified Eagle medium

(DMEM) supplemented with 10% of fetal bovine serum (Sigma-Aldrich, St. Louis, MO, F6178), 100 U/ml penicillin along with 100 µg/ml streptomycin (Gibco, Waltham, MA, 15070) and 2.5 g/ml amphotericin B (Gibco, 15290) at 37°C in a humidified 5% CO₂ incubator. For the Vitamin C treatment, 4 × 10⁵ cells per well were seeded into six-well plates and supplemented for 72 hr with 50 µg/ml Vitamin C (Sigma-Aldrich, St. Louis, MO, A7506). For the HDAC inhibitor suberoylanilide hydroxamic acid (SAHA) treatment (Sigma-Aldrich, SML0061), cells were seeded at 60% of confluence and the experiment was carried out at 10 µM for 48 hr.

Cell proliferation and cell viability assays

Cell proliferation rates were established using the xCELLigence Real-Time Cell Analysis system (RTCA, ACEA Bioscience, San Diego, CA) and represented by Cell Index parameter. A total of 15,000 empty or stably-transfected LN229 clone cells were seeded onto xCELLigence multiwell plates (E-Plate L8 PET 00300600870) and cell impedance measurements were acquired every 2 hr for 8 consecutive days (detailed information at <https://www.aceabio.com/wp-content/uploads/CIM-Protocol.pdf>). Cell viability was determined by MTT (3-(4,5-dimethylthiazol-2-yl)-2,5-diphenyltetrazolium bromide) assay on cell clones stably transfected with TET3 or empty vectors. Twelve replicates per condition and time point were estimated. Absorbance at 595 nm was measured with the automated microtiter plate reader Synergy HT (BioTek, Winooski, VT). Cell death was estimated with the FITC-Annexin V staining kit (Biolegend, San Diego, CA), following the manufacturer's instructions. Briefly, empty and stably transfected TET3 clone cells were seeded at 70–80% of confluence. Apoptosis levels were measured at different time points (every 24 hr for 10 days), and the cell culture underwent some spontaneous apoptosis in the course of proliferation due to the high cell density throughout the experiment. Cell cycle analysis was conducted by flow cytometry using propidium iodide (Sigma, P4170) at different time points (every 24 hr for 10 days).

Xenograft models

For the xenograft experiments, 750,000 cells (empty and TET3 stably transfected clones) were subcutaneously injected into each flank of 5-week-old nude mice (*n* = 5; Charles River, NU/NU). Cells were injected suspended in 0.1 ml DMEM mixed with 1:2 Matrigel Matrix High Concentration (Cat No 354248). Tumor volumes were measured with a caliper twice per week and calculated using the following formula: $V = 4/3\pi(Rr)^2$. After animal sacrifice, the monitored tumors were excised and weighed.

Computational analyses

Detailed information related to DNA methylation and gene expression arrays, region set enrichment calculations, survival data and other types of statistical analyses are available at the "Supplementary experimental procedures" section.

Data availability

Raw methylation HumanMethylationEPIC files including empty and TET3 overexpression experiments in LN299 cells were deposited in ArrayExpress under the accession number E-MTAB-6001.

Accession numbers

Accession numbers for HumanMethylation450K arrays were obtained from E-MTAB-6003 and GSE73895. Whole genome bisulfite sequencing (WGBS) dataset was obtained from E-MTAB-5171. Raw data corresponding to gene expression arrays were acquired from GSE14805, GSE83130, E-GEOD-36634, E-GEOD-15824, E-GEOD-23806, GSE75945, GSE29796 and GSE4412. Accession numbers for RNA sequencing analyses were obtained from the SRA database studies SRP113619, SRP173011 and SRP095447.

Supplementary experimental procedures

Detailed information on the primer sets used in our study is included in Supporting Information Table S2. In-depth description of quantitative reverse transcription polymerase chain reaction (RT-qPCR) conditions, colony formation assays, immunofluorescence, immunohistochemistry and other molecular techniques are available as Supplementary Data at International Journal of Cancer's website. Supporting Information Figures and Tables have been uploaded to Zenodo under the doi number 10.5281/zenodo.3240296.

Results

TET3 is epigenetically repressed in glioma

To identify possible epigenetic alterations of *TET3* in glioblastoma we analyzed 5mC and 5hmC data obtained with the Infinium HumanMethylation450K BeadChip platform and determined the levels of these two epigenetic modifications in promoter and intragenic CpG sites in five nontumorigenic brain samples, and nine samples obtained from glioblastoma patients (E-MTAB-6003).²⁵ Levels of 5mC and 5hmC were locus-dependent and significantly differed between normal brain tissue and glioma samples (Fig. 1a, Supporting Information Fig. S1). In control brain, absolute levels of 5hmC in most of the CpG sites analyzed oscillated between 10 and 30%, while, on the contrary, levels of 5hmC in glioma samples were almost undetectable in most of the CpG sites analyzed (Fig. 1a). These observations were further confirmed using a recent publicly available 450K dataset (GSE73895),²⁶ along with additional high-throughput data obtained from WGBS experiments (E-MTAB-5171)²⁷ (Supporting Information Fig. S1 and Table S3). It is worth highlighting that aberrant DNA methylation patterns were also detected in the other TET family members, that is, the *TET1* and *TET2* genes. Whilst the extent and location of these changes varied in a gene-specific manner, a global gain of 5mC and a global reduction of 5hmC levels were observed for most of the glioma samples (Supporting Information Fig. S1 and Table S3),

indicating the global impairment of the DNA methylation status in the context of the tumor.

We next used bisulfite pyrosequencing to technically validate the methylation array data (E-MTAB-6003) at one promoter (cg11236515) and two intragenic CpG sites (cg03763077 and cg15996154) of the *TET3* gene (Fig. 1c). In addition, we analyzed the level of 5mC and 5hmC at the same CpG sites in an independent cohort of 12 control brains (six gray matter

and six white matter) and 12 gliomas (Supporting Information Fig. S2). In general, absolute levels of 5mC and 5hmC were similar to the levels observed with the methylation arrays. To discard any potential bias concerning the experimental oxidation procedure, the loss of 5hmC in glioblastoma was thoroughly validated using an alternative technique based on DNA immunoprecipitation with an antibody against 5hmC (Supporting Information Fig. S2G). The results indicated that

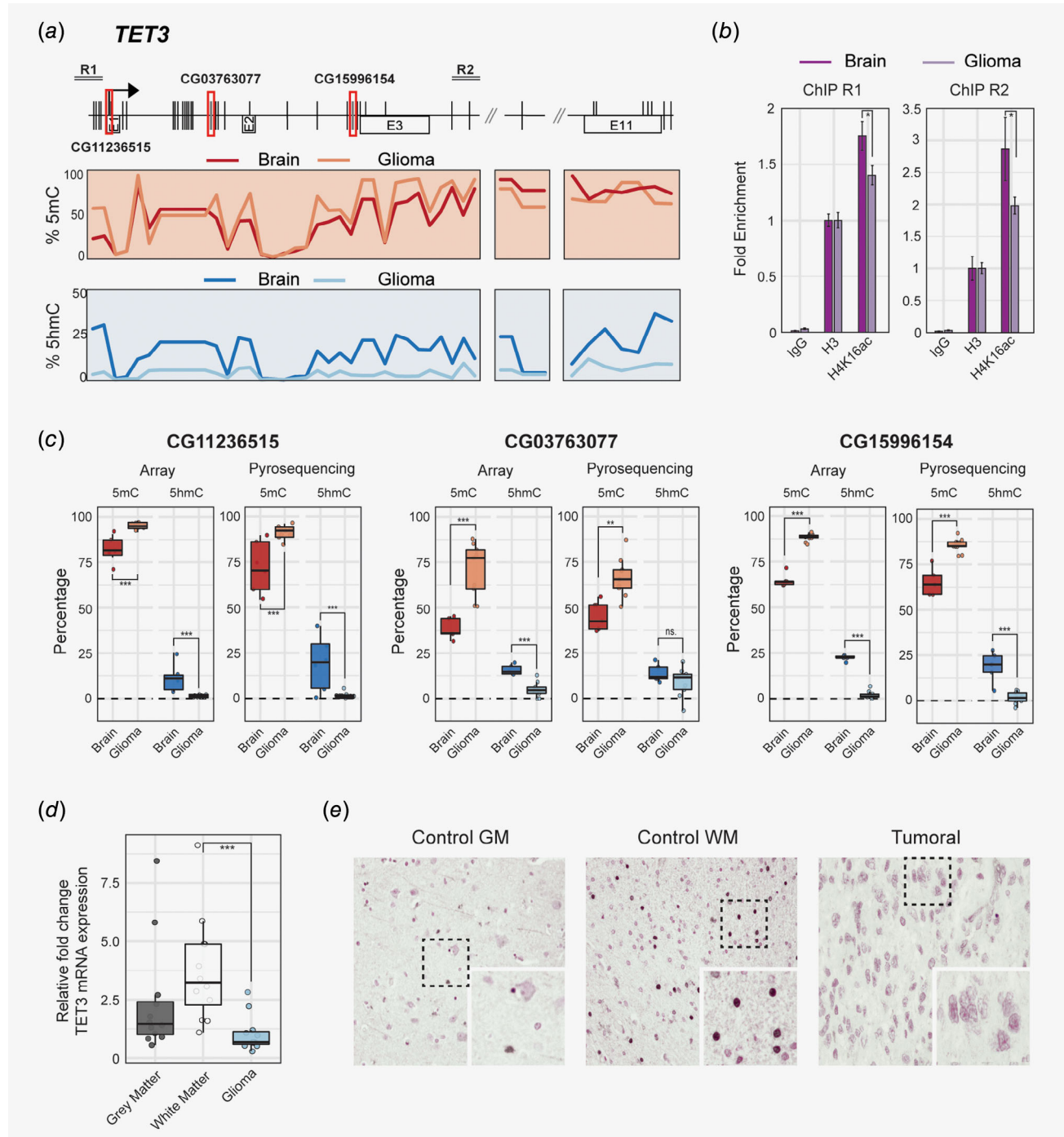


Figure 1. Legend on next page.

levels of 5hmC were lower at these sites in all the gliomas analyzed as compared to the control brains, demonstrating that loss of *TET3* hydroxymethylation and gain of 5mC are frequent phenomena in brain tumors.

To identify other possible epigenetic mechanisms involved in *TET3* regulation we performed *in vitro* and *in silico* analyses on a set of seven classically studied histone marks. First, we performed quantitative chromatin immunoprecipitation (ChIP) analyses using an antibody against H4K16ac, a histone posttranslational modification associated with gene activation,²⁸ and frequently impoverished in human cancer.²⁹ We found a consistent and significant decrease of H4K16ac levels in the promoter and gene body of *TET3* (Fig. 1b). To explore other potential sources of epigenetic downregulation, we analyzed publicly available data on five activating and one repressive histone marks (H3K4me1, H3K4me3, H3K9ac, H3K27ac, H3K36me3 and H3K9me3) corresponding to Brain Inferior Temporal Lobe and Brain Dorsolateral Prefrontal cortex samples from the NIH Roadmap's consortium,³⁰ and the status of the same set of histone marks in two glioblastoma samples obtained from a patient-derived glioblastoma model (GSE113816).³¹ In the case of the *TET3* gene, we observed a dramatic decrease in the signal of epigenetic marks associated with promoter activation (H3K4me3 and H3K9ac), transcriptional elongation (H3K36me3) and active enhancers (H3K4me1 and H3K27ac) in the context of the tumor (Supporting Information Fig. S3). Notably, we observed a similar epigenetic downregulation for other *TET* genes, and this was particularly associated with active promoters (H3K4me3 and H3K9ac). These results further support the notion that, in addition to DNA methylation and DNA hydroxymethylation, global aberrations in histone posttranslational modifications might play an important role not only in *TET3* regulation but also in the regulation of other *TET* genes in glioma.

Altered levels of 5mC/5hmC and loss of activating histone marks are associated with *TET3* gene downregulation

To delve deeper into the possible effects of the aforementioned epigenetic alterations in *TET3* expression, we first measured

TET3 mRNA levels in 12 control brains (12 gray matter and 12 white matter paired samples) and 11 primary gliomas. These experiments revealed that *TET3* mRNA was downregulated in most of the cancer samples as compared to healthy tissue (Wilcoxon rank sum test, *p*-value <0.001) (Fig. 1d). In addition, these results were comprehensively validated using additional gene expression arrays and RNAseq datasets generated by the TCGA consortium (Supporting Information Fig. S4 and Table S4). Interestingly, *TET3* mRNA levels were significantly reduced in TCGA-GBM samples, with the exception of the G-CIMP and proneural subtypes, which, as well as expressing higher levels of *TET3*, were also associated with better prognosis of GBM patients (Supporting Information Fig. S4). In this same vein, the downregulation of other genes from the *TET* family has also been observed in glioma samples and glioblastoma cell lines (Supporting Information Fig. S5 and Table S5) when compared to normal brain tissue data obtained from other publicly available sources.^{32–35}

To validate these observations at the protein level, we analyzed the expression of *TET3* protein in control brain and glioblastoma samples by immunohistochemistry and confirmed that, in accordance with mRNA expression data, normal brain presents higher expression of *TET3* protein than tumoral samples (Fig. 1e and Supporting Information Fig. S6).

To explore in more depth the relationships between the epigenetic alterations described above and *TET3* downregulation, we used two pharmacological treatment approaches. First, we incubated LN229 glioblastoma cells with Vitamin C (50 µg/ml), a treatment that has been shown to increase 5hmC levels.²⁰ Use of this drug-induced *TET3* expression (Fig. 2b) (General linear model [GLM] *p*-value <0.01) and slightly increased 5hmC while reducing 5mC levels at the CpG sites cg11236515 and cg03763077 (Fig. 2c). In addition, we incubated the same glioblastoma cell line with suberoylanilide hydroxamic acid (SAHA), an inhibitor of the histone deacetylases HDAC1 and HDAC2.³⁶ SAHA treatment significantly enhanced *TET3* expression (Fig. 2d; GLM *p*-value <0.001) and showed an increase of histone H4K16 acetylation levels at specific *TET3* regions (Fig. 2e; GLM *p*-value <0.01). The efficiency of the Vitamin C and SAHA

Figure 1. Altered levels of DNA methylation and reduction of H4K16ac mark are correlated with *TET3* gene expression. (a) Line plots depict percentage of averaged methylation values of *TET3* methylated (red) and hydroxymethylated (blue) CpG regions in control brain and glioma samples. Data were generated from a genome-wide DNA methylation analysis performed with the Infinium HumanMethylation450K platform (E-MTAB-6003). Upper diagram indicates the relative location across the gene body of *TET3* of the CpGs analyzed in the array or the ChIP amplicons interrogated in the H4K16ac immunoprecipitation experiment. (b) H4K16ac relative fold enrichment at *TET3* regions estimated by ChIP assay in brain and glioma tissues. Immunoprecipitations were performed using antibodies against H4K16ac, total histone H3 as positive control and IgG antiserum as negative control. Quantitative real-time PCR analysis was performed for *TET3* specific regions, and all measurements were performed in triplicate. Relative enrichments were calculated using the $\Delta\Delta Ct$ method, and data were normalized firstly against IgG and then relativized against H3. (c) Box plots (left) representing 5mC and 5hmC array data corresponding to *TET3* probes cg11236515, cg03763077 and cg15996154 in five control brain and nine glioblastoma samples. Box plots (right) illustrate validation of cg11236515, cg03763077 and cg15996154 *TET3* CpG sites performed through pyrosequencing experiments using the same set of normal brain and glioma samples. *p* Values indicated were adjusted by applying the Bonferroni correction. (d) Box plot depicting *TET3* mRNA expression in 12 gray matter and 12 white matter samples compared to 11 glioblastoma samples, as measured by qRT-PCR. Wilcoxon rank sum tests were applied and *p* values were adjusted by applying the Bonferroni correction. (e) Representative images of white and gray matter immunohistochemical stainings with *TET3* antibody. White matter presents positive *TET3* nuclear staining in contrast with tumoral sections, which essentially display background levels of *TET3*. Magnification: 20x.

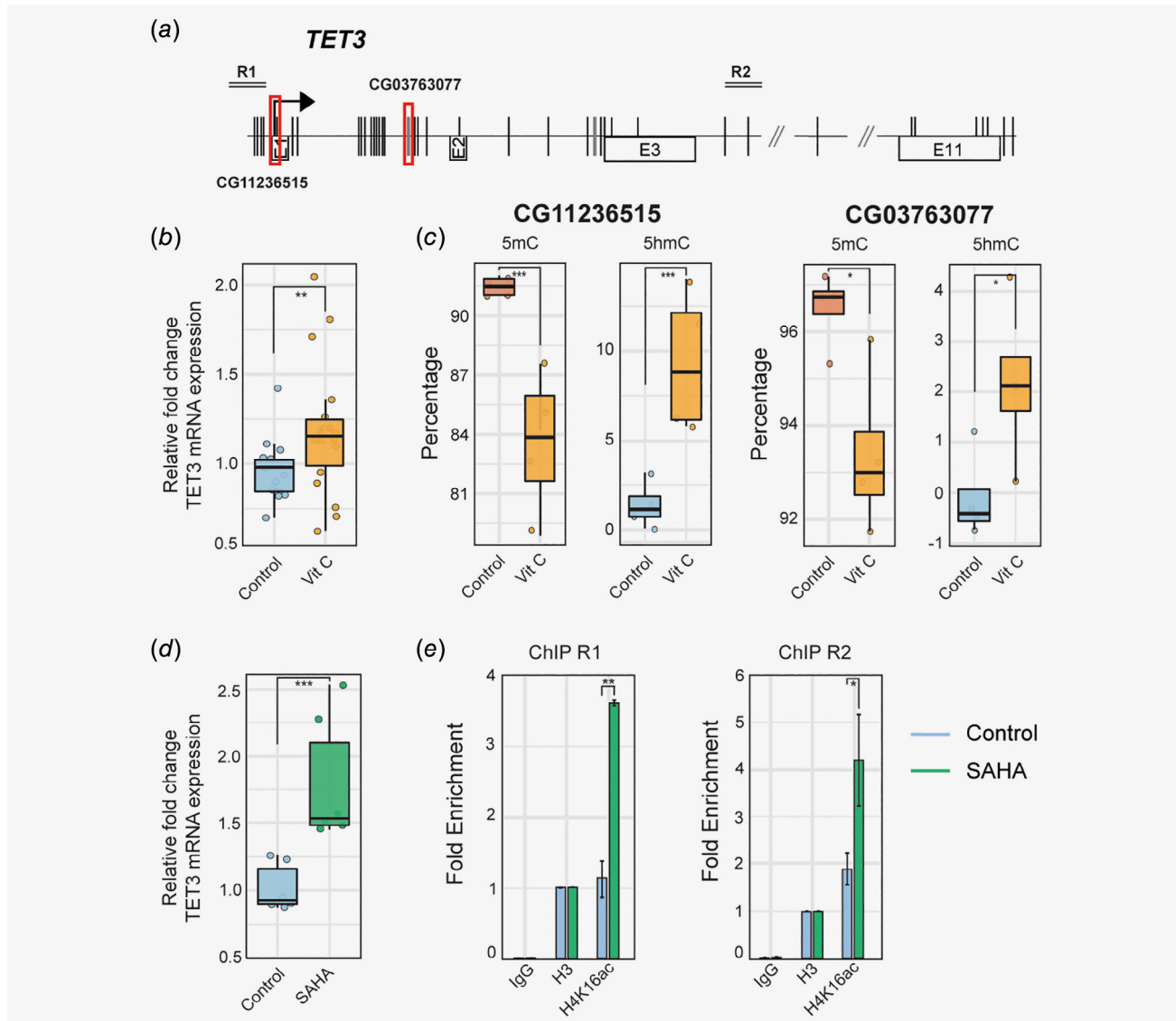


Figure 2. Pharmacological restoration of 5hmC or H4K16ac levels induces *TET3* expression. (a) Diagram illustrates the relative location of the ChIP amplicons interrogated in the H4K16ac immunoprecipitation experiment and the CpG probe analyzed across the gene body of *TET3*. (b) Box plot showing the relative mRNA levels of *TET3* in LN229 cells supplemented with 50 µg/ml Vitamin C for 72 hr, estimated from nine biological replicates generated in two independent experiments. (c) Box plots depicting methylation and hydroxymethylation levels estimated by pyrosequencing in LN229 cells supplemented with Vitamin C at the CpG sites cg11236515 and cg03763077. Results were obtained from two independent experiments performed in duplicate. (d) Bar graph representing *TET3* mRNA relative expression levels of LN229 cells treated with 10 µM SAHA for 48 hr. (e) Bar graph depicting H4K16 levels estimated by ChIP assay in LN229 supplemented with SAHA at *TET3* specific region. Results were obtained from two independent experiments performed in triplicate. This data confirm that while Vitamin C enhances 5hmC and SAHA increases H4K16ac levels, both treatments activate *TET3* expression. GLMs were used for statistical comparisons. For all statistical analyses, asterisks indicate the degree of statistical significance (**p-value <0.001; **p-value <0.01; *p-value <0.05).

treatments was confirmed by dot blot and high-performance liquid chromatography/high-performance capillary electrophoresis analyses of global histone H4 acetylation, respectively (Supporting Information Fig. S7). Collectively, these results indicate that these epigenetic alterations promote *TET3* downregulation at both the mRNA and protein level in glioblastoma, both *in vitro* and *in vivo*.

Restoration of *TET3* impairs tumor growth of glioma cells *in vitro* and *in vivo*

To study the functional role of *TET3* epigenetic downregulation in glioma, we stably transfected a *TET3* protein expression vector into the glioblastoma cell line LN229, which shows low hydroxymethylation and expression levels of *TET3*. *TET3* mRNA expression in stably-transfected clones was

confirmed by qRT-PCR (GLM *p*-value <0.01; Fig. 3*a*) and western blot (Supporting Information Figs. S8A and S8B). Further confirmation was provided by the increased overall hydroxymethylation levels observed for *TET3* in *TET3* stably transfected cells compared to control LN229 cells (Fig. 3*b*). Importantly, *TET3* restoration did not affect the expression of other TET members in our experimental model (Supporting Information Fig. S8C), indicating that these effects were not confounded by any potential compensatory mechanism related to other TET factors. Impedance-based cellular growth assays revealed that *TET3*-transfected cells grew less than control cells (GLM *p*-value <0.01; Fig. 3*c*). Supporting this, MTT analyses showed that *TET3* upregulation resulted in reduced cell viability (GLM *p*-value <0.001) (Fig. 3*d*). Next, we used colony formation assays to determine the role of *TET3* in the capacity of glioblastoma cells to produce progeny. The results showed that *TET3* overexpression induced a ~40% reduction in colony formation ability (GLM *p*-value <0.001) (Fig. 3*e*). However, the detailed analysis of apoptosis and cell cycle under these conditions revealed that reduced growth and viability were not caused by increased levels of apoptosis, and only minor differences in cell cycle distribution were observed between *TET3* transfected and control cells (Figs. 3*f* and 3*g*).

To explore the differentiation potential of these cell clones, we performed neural differentiation profiling on *TET3* restoration (Supporting Information Fig. S8D). We observed an overall increase in the expression of genes related to embryonic stem cell and neural stem cell development, as well as genes essential for the establishment of peripheral neurons. In contrast, increase in *TET3* levels impaired the expression of genes involved in oligodendrocyte, motoneurons and Schwann cell development, and induced the marked downregulation of genes associated with neuron-restricted progenitors (Supporting Information Fig. S8D). Some of these observations were validated by means of other orthogonal approaches, as was the case for SOX2 (neural progenitor factor), which had higher signal intensities in *TET3* overexpressing cells (Fig. 3*h* and Supporting Information Fig. S8). These experiments suggest that the differences in cellular growth might be partially mediated by a cell differentiation process, as has been recently described by Zhang *et al.*³⁷

To further characterize the role of *TET3* downregulation *in vivo*, we subcutaneously injected *TET3*-overexpressing cells and control cells transfected with empty vector into immunodeficient nude mice. As expected, control cells displayed exponential growth. In contrast, *TET3*-overexpressing cells did not generate exponentially growing tumors (Wilcoxon rank sum test, *p*-value <0.01; Figs. 3*i* and 3*j*). At the time of sacrifice (63 days), the average weight of tumors originated from *TET3*-overexpressing cells was less than 0.1 g, while those from control cells weighed a median of 0.6 g (Wilcoxon rank sum test, *p*-value <0.05; Fig. 3*k*). These results thus indicate that restoration of *TET3* activity in glioblastoma cells reduces tumorigenicity *in vitro* and *in vivo*.

TET3 overexpression partially restores the 5hmC levels observed in human brains

To gain further insights into the downstream effects that may occur upon *TET3* overexpression, we performed genome-wide DNA methylation analyses to characterize the extent of 5mC and 5hmC in the human glioma cell line LN229. We also compared our results with recent DNA methylation data from human brains and gliomas (E-MTAB-6003)²⁵ (Fig. 4). Global levels of 5mC were slightly reduced in human brains as compared to their tumorigenic counterparts and the range of these changes was barely detectable in our *TET3* transfected background (Fig. 4*a*). Interestingly, 5hmC levels were both substantially increased in brain and *TET3* transfected LN229 cell line as compared to human glioma and control cell line, respectively.

We next identified a total of 30,355 autosomal CpG sites that were differentially hydroxymethylated (dhmCpGs) between brain and glioma samples (false discovery rate <0.05, differences in methylation >15%, Supporting Information Table S6), and 18,711 dhmCpGs between *TET3* transfected LN229 cells as compared to their empty analogues (differences in methylation >25%, Supporting Information Table S7) (Fig. 4*b*). The distribution of 5hmC levels vs. their corresponding 5mC signals was considerably anticorrelated in brain and in *TET3* transfected cells compared to their related controls, while the observed displacement toward increased levels of 5hmC was similar in both scenarios (Fig. 4*c*, top). On the contrary, both glioma and control LN229 cells display marginal levels of 5hmC in these same dhmCpG sites (Fig. 4*c*, bottom).

With regard to the genomic distribution of significant 5hmC loci in normal brain, these dhmCpGs were enriched at open sea locations (Fisher's exact test, *p*-value <<< 0.001, odds ratio [OR] = 1.30), as well as intronic and distal promoter regions (Fisher's exact test, *p*-value <<< 0.001, OR = 1.55 and *p*-value <<< 0.001, OR = 1.57, respectively). Moreover, brain dhmCpGs were clearly impoverished in CpG islands (Fisher's exact test, *p*-value <<< 0.001, OR = 0.24) and promoter regions (Fisher's exact test, *p*-value <<< 0.001, OR = 0.37) as compared to the Illumina 450K background array distribution (Fig. 4*d*). On the other hand, dhmCpGs from *TET3* transfected LN229 cells only displayed a slight reduction in CpG island distribution (Fisher's exact test, *p*-value <<< 0.001, OR = 0.89) and promoter regions (Fisher's exact test, *p*-value <<< 0.001, OR = 0.42), and there was a modest increase in distal promoters and intronic sites (Fisher's exact test, *p*-value <<< 0.001, OR = 1.42 and *p*-value <<< 0.001, OR = 1.16, respectively). These results suggest that, although the global restoration of 5hmC levels upon *TET3* overexpression in LN229 cells sounds efficient, the targeted genomic location of dhmCpGs in normal brains vs. glioblastoma cell lines might appreciably differ.

***TET3*-mediated 5hmC is associated with H3K4me1 and enhancer elements**

To get more insights into the potential discrepancies in the results presented above, we sought to determine whether

5hmC deposition caused by TET3 overexpression might have a common nexus with the brain tissue background. We performed chromatin enrichment analyses by combining our 5hmC data with publicly available datasets from encyclopedia of DNA elements (ENCODE) and the NIH Roadmap Epigenome consortia.^{30,38} In doing so we observed a significant enrichment of dhmCpGs from brain and TET3 transfected

LN229 cells in embryonic stem (ES) cells and brain genomic regions decorated with the histone mark H3K4me1 (Supporting Information Fig. S9A and S9B). However, TET3-mediated 5hmC in LN229 overexpressing cells was also substantially enriched at H3K36me3 and H3K27me3 histone modifications (Supporting Information Fig. S9B), suggesting the existence of a broader effect in those genomic loci related to gene bodies and

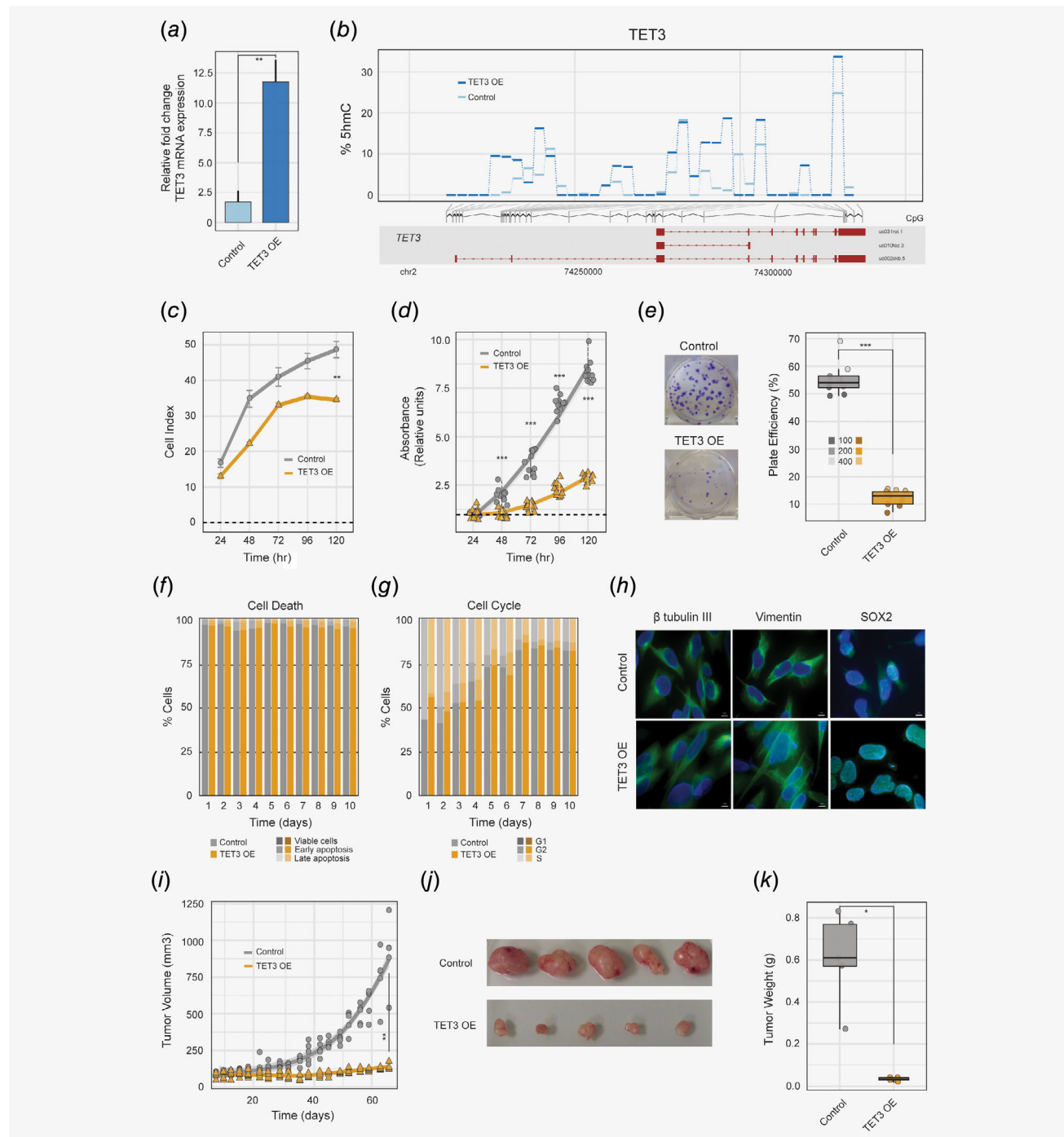


Figure 3. Legend on next page.

the deposition of Polycomb complex. Indeed, further comparisons with publicly available chromatin segmentation data,³⁰ which integrate the previously mentioned combination of histone modifications in order to describe a combinatorial and spatial pattern of chromatin states, confirmed that TET3-mediated 5hmC in LN229 cells was significantly enriched at Polycomb-repressed regions (Supporting Information Fig. S9D). Nonetheless, our results also indicated that both brain and TET3 modulated dhmCpG sites were enriched in active and genic enhancer elements (Supporting Information Fig. S9C and S9D), at least in the case of brain-related tissues, suggesting that the phenotype observed upon TET3 overexpression in LN229 cells might be partially mediated by a common set of chromatin signatures.

Functional characterization of TET3-mediated 5hmC in human glioblastoma cells

To study the functional connections between 5hmC levels in glioblastoma cells, we compared the previously identified dhmCpGs in brain vs. glioma samples and TET3 transfected LN229 cells vs. their control counterparts. Interestingly, 907 common dhmCpG sites were shared between both conditions, indicating a small, but substantial overlap in hydroxymethylated loci (Fig. 5a; Enrichment score 1.6, expected hits = 594, hypergeometric test *p*-value << 0.001). Gene ontology (GO) analyses of genes containing dhmCpGs revealed a significant enrichment in common biological processes related to axon development and axonogenesis (Fig. 5b, left). Furthermore, a detailed inspection of the common Kyoto Encyclopedia of Genes and Genomes (KEGG) and Reactome signaling pathways that were significantly hydroxymethylated in both brain and TET3 overexpressing cells indicated a potential regulatory role for this process in Rap1 and NGF signaling cascades.

Recent work has demonstrated that downregulation of the TLX gene induces TET3 expression and inhibits glioblastoma stem cell self-renewal and tumorigenesis.²⁴ To identify candidate target genes which may be involved in the reduced proliferation effects observed in TET3 transfected LN229 cells, we obtained genome-wide expression data from available databases (see Materials and Methods and Supporting Information Data section) and we analyzed the antagonistic expression outcomes of TET3 and TLX knockdown conditions in human primary glioblastoma stem cell lines. In order to focus solely on those direct gene expression changes potentially mediated by TET3 activity, we compared genes that were significantly altered but displayed opposing gene expression trends upon TET3 or TLX shRNA treatment (Fig. 5c, Supporting Information Table S8). We then intersected the list of gene expression candidates with our list of common hydroxymethylated genes in brain and TET3 transfected LN229 cells (Fig. 5c).

Interestingly, we found that *RECK*, *LTPB1*, *CYS1* and *WBP1L* genes all display elevated 5hmC levels in normal brain and TET3 overexpressing cells, but also manifest opposite gene expression trends upon antagonistic TLX and TET3 knockdown conditions. Overall levels of 5hmC were clearly diminished in gliomas and LN229 cells as compared to TET3 overexpressing cells and brain tissue (Fig. 5d). Moreover, the expression of these genes was mainly correlated with *TET3* expression, with the exception of *WBP1L*, which was anti-correlated with *TET3* / 5hmC levels (Fig. 5e).

A detailed exploration of the genomic boundaries of *RECK* and *WBP1L* allowed us to identify a pattern in the global hydroxymethylation of CpGs along the gene body of these candidate genes in both brain and TET3 transfected LN229 cells (Supporting Information Fig. S10A and S10B). Interestingly, these intragenic 5hmC arrangements were severely

Figure 3. TET3 overexpression impairs *in vitro* cell proliferation and restrains tumor growth of glioma cells *in vivo*. (a) Bar graph showing *TET3* mRNA relative expression levels of LN229 cells transfected with *TET3* expression vector (full coding sequence) vs. empty control. (b) Analysis of overall hydroxymethylation levels observed for *TET3* in *TET3* transfected and empty LN229 cells, obtained with the HumanMethylationEPIC platform. 5hmC levels were considerably increased in *TET3* overexpressing clones compared to control cells. (c) *In vitro* growth characterization of *TET3* transfected LN229 cells. Real-time impedance of LN229 cells was obtained using E-Plates and xCELLigence RTCA instruments, and by monitoring empty and *TET3* stably transfected clones after seeding 15,000 cells (in triplicate). Cell proliferation is represented using the Cell Index (CI) parameter (y-axis) per time unit interval (x-axis). Impedance-based cellular growth assays revealed that *TET3* overexpressing cells present diminished cell growth in comparison with empty control. (d) Characterization of *in vitro* cell viability was determined by MTT assay on control and *TET3* transfected cells. Twelve replicates per condition and time point were estimated. (e) Colony formation assay was conducted by seeding cells at different densities (100, 200 and 400 cells). Results are represented in the box plot as plate efficiency (PE = [number of colonies formed/number of cells seeded] × 100), calculated from three independent replicates for each of the densities. GLMs were applied in all the previous experiments and *p*-values were adjusted applying the Bonferroni correction. (f) Apoptosis assays were conducted in empty and *TET3* stably transfected clones and bar plots represent the percentage of cells in the early and late apoptosis stages which were detected by the FITC-Annexin V staining kit over the course of 10 days. The experiment was performed analyzing each time point in duplicate. (g) Cell cycle analysis was conducted by flow cytometry using propidium iodide (PI) at the previously mentioned time points and carried out in duplicate. Bar graph illustrates the mean percentage of cells in G1, S and G2 stages obtained in two independent experiments. (h) Immunofluorescence staining for Tubulin beta-3 chain (β tubulin III), Vimentin and SOX2 (green) in empty and *TET3* transfected cells. SOX2 (neural progenitor factor) and Vimentin signals are enhanced in overexpressing *TET3* cells. (i) *TET3* expression impairs *in vivo* tumor growth. Immunodeficient nude mice (*n* = 5) were injected on each flank with empty (gray) and *TET3* transfected LN229 cells (orange). Evolution of tumor growth measured as tumor volume is shown. (j) Subcutaneous tumors isolated after animal sacrifice are shown. (k) Evolution of tumor growth, measured as tumor weight, after animal sacrifice. LN229 control cells produced significantly increased tumor volumes and weights in nude mice. Wilcoxon rank sum tests were applied and *p* values were adjusted by applying the Bonferroni correction. For all statistical analysis ****p*-value < 0.001; ***p*-value < 0.01; **p*-value < 0.05.

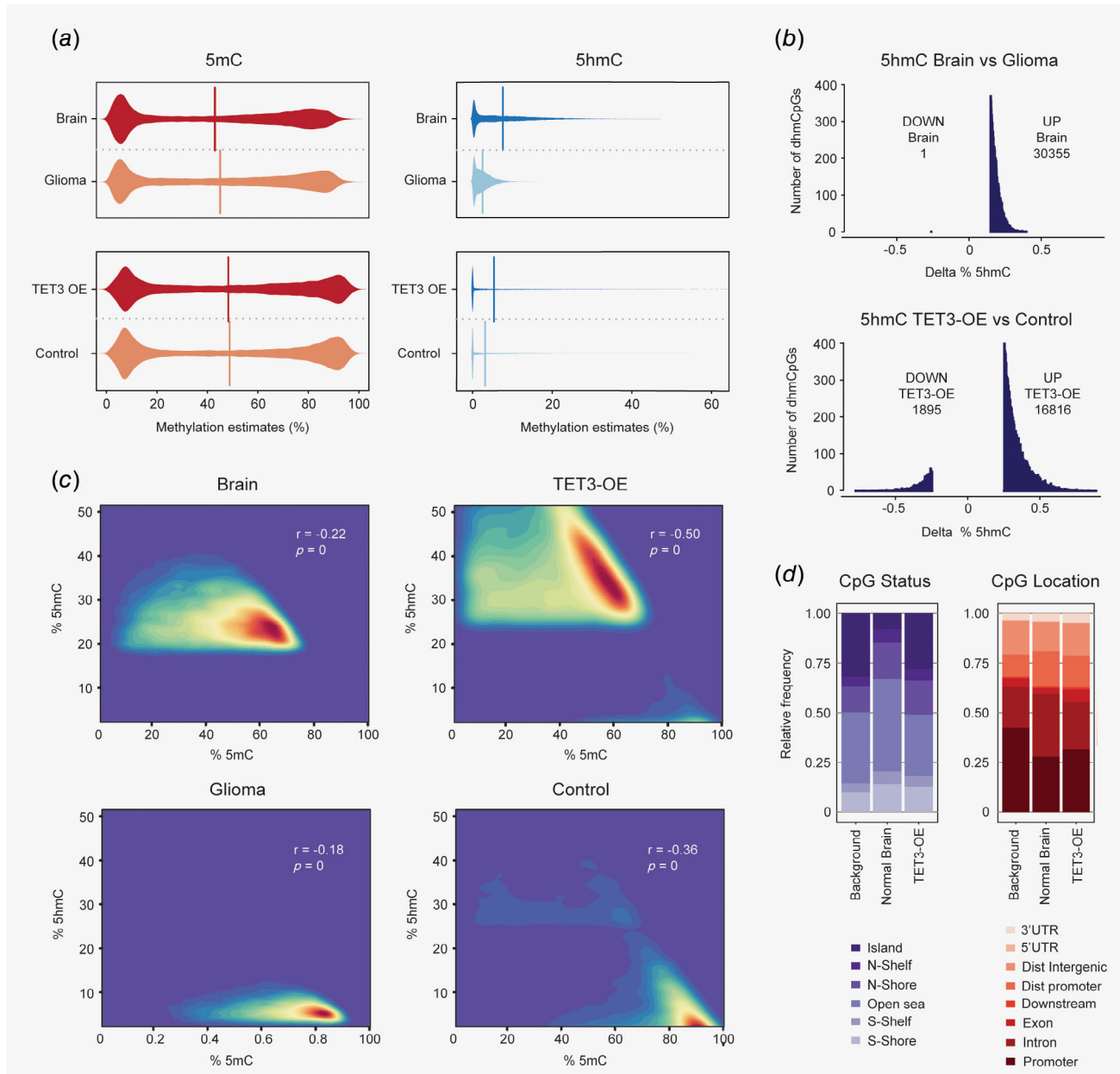


Figure 4. Partial restoration of brain 5hmC levels upon TET3 overexpression in LN229 cells. (a) Genome-wide DNA methylation analysis performed with the Infinium HumanMethylation450 and Infinium MethylationEPIC platforms. Violin plots depict overall methylation estimates of 5mC (left) and 5hmC (right) measurements in brain and glioma samples (top, brain, $n = 5$; glioma, $n = 11$) or LN229 cells overexpressing TET3 vs. empty control (bottom). Vertical lines indicate the median value for each of the above-mentioned distributions. (b) Number of dhmCpGs obtained from the brain vs. glioma (top), or the TET3 transfected cells vs. control (bottom) comparisons. Histograms indicate the number of dhmCpGs (y-axis) per unit interval (x-axis), calculated as the difference of 5hmC percentages between either brain vs. glioma, or LN229 cells overexpressing TET3 vs. empty control. UP and DOWN counts represent the number of probes that displayed more or less, respectively, hydroxymethylation in each of the comparisons. (c) Restoration of 5hmC levels in TET3 transfected cells. Heat density scatterplots demonstrate the global redistribution of 5hmC levels in brain and TET3 overexpressing LN229 cells at those genomic loci previously marked with 5mC in glioma or LN229 control cells (brain and glioma, $n = 30,355$; TET3 transfected and control, $n = 16,816$). Pearson product-moment correlation coefficients (r) between the percentages of 5hmC and 5mC are indicated for each case. All comparisons are statistically significant ($p \ll 0.001$). (d) CpG status and CpG location of significant 5hmC sites. Stacked barplot illustrates the relative proportion of the different CpG statuses (left) or CpG locations (right) in the context of the background distribution of the Infinium HumanMethylation450 array platform, and the significant 5hmC probes obtained from normal human brain and TET3 transfected cells, respectively. In the latter cases, the probes common to both the EPIC and the 450K platforms were selected for legitimate representation purposes.

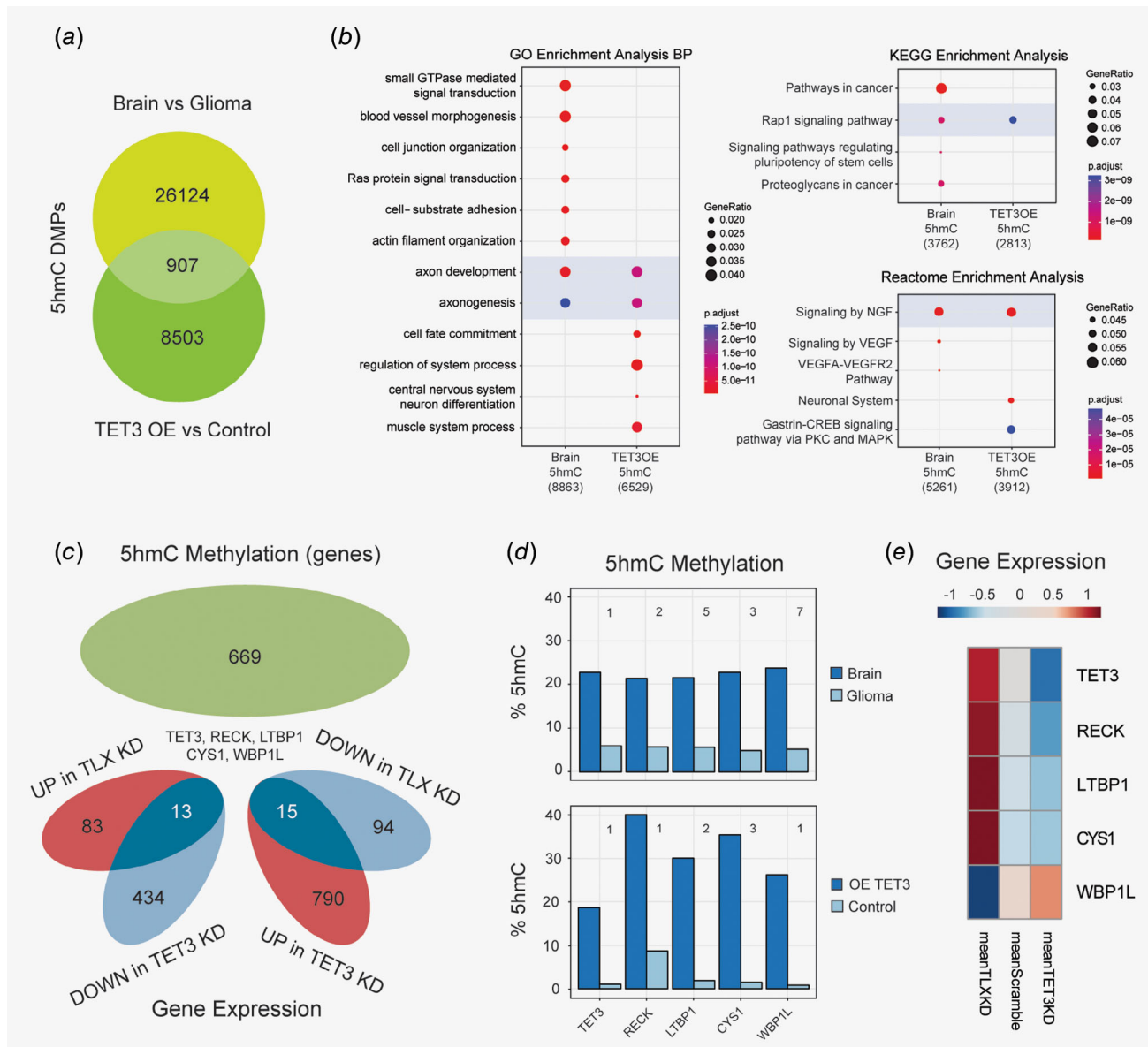


Figure 5. Molecular pathways and candidate genes affected by TET3-mediated 5hmC. (a) Overlap between dhmCpGs in brain vs. glioma, and in TET3 transfected vs. empty LN229 cells. Only hydroxymethylated probes common to both the 850K and the 450K Illumina methylation platform were considered for legitimate comparisons. Numbers indicate the amount of significant 5hmC sites in each experimental context. (b) Gene, KEGG and Reactome Ontology enrichment analyses. The number of significant dhmCpGs obtained for brain and for TET3 overexpression was used for downstream purposes. Numbers displayed below conditions indicate the amount of genes with dhmCpGs and circle sizes represent the ratio between the number of identified hits and the number of total hits in a given category. Color range indicates the significance of the observed ontology by means of the adjusted p-value. (c) Overlap between hydroxymethylated genes common to brain and TET3 transfected LN229 cells (green oval), and genes with altered gene expression in primary human glioblastoma stem cell (GSC) lines upon knockdown of TET3 or TLX. Gene expression datasets were obtained from GSE75945. Highlighted genes represent candidate targets with significant changes in 5hmC and antagonistic gene expression patterns between TLX/TET3 KD treatments. (d) 5hmC levels of *RECK*, *LTBP1*, *CYS1* and *WBP1L* in brain and glioma samples (top) and TET3 transfected and control LN229 cell lines (bottom). Y-axis represents the mean percentage of 5hmC levels taking into consideration the significant dhmCpGs identified for each of the target genes. Number of significant 5hmC probes per gene are indicated. (e) Gene expression levels of *TET3*, *RECK*, *LTBP1*, *CYS1* and *WBP1L* in primary human GSC lines upon TLX ($n = 2$) or TET3 ($n = 4$) depletion (control cells, $n = 4$). Heatmap indicates relative fold change in gene expression values, calculated as the average signal between all the samples and the collapsed transcript probes for a given candidate gene contained in the GeneChip PrimeView Human Gene Expression Array platform (Affymetrix).

impaired in glioma samples and control LN229 cells. Overall, these results indicate that differential 5hmC levels mediated by TET3 activity might have a functional impact on gene

expression in glioma, especially in the case of *RECK*, *LTBP1*, *CYS1* and *WBP1L* genes, which display an altered 5hmC pattern in LN229 cells and tumor samples.

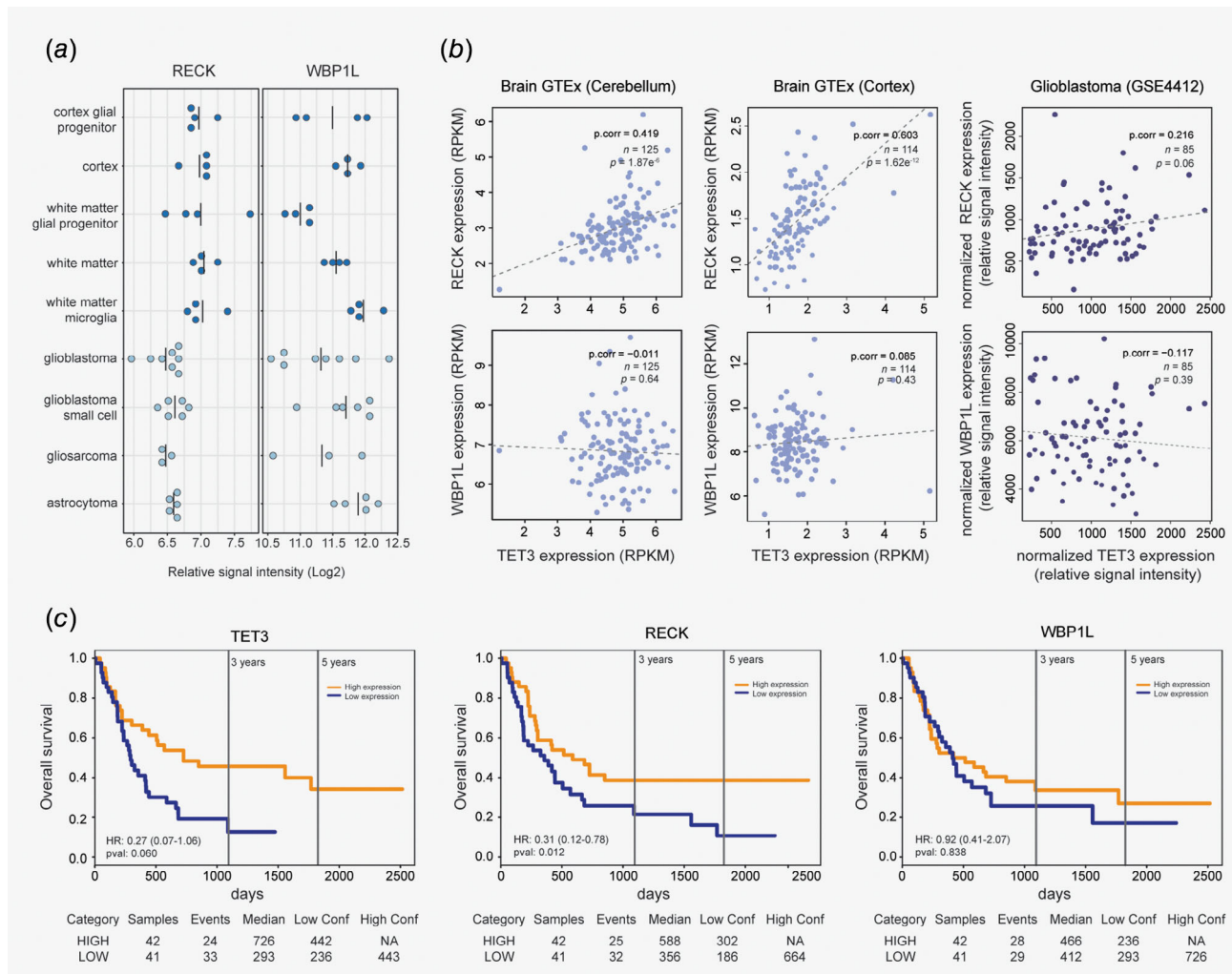


Figure 6. Expression of *TET3* and *RECK* genes is correlated with better prognosis of GBM patients. (a) *RECK* and *WBP1L* expression in normal or brain cancer samples. Dotplot indicates the log₂ relative expression level of *RECK* or *WBP1L* in samples from brain cortex and white matter (dark blue), or samples obtained from brain tumors (light blue, datasets correspond to GSE29796). For each sample, illustrated as single dots, the mean value of the collapsed array probes for the different genes is shown. (b) Correlation between *TET3* and *RECK* or *WBP1L* gene expression in normal brains or glioblastoma patients. Scatterplots depict robust correlation scores between *TET3* and *RECK*, or between *TET3* and *WBP1L* pairwise comparisons. Normal cortex and cerebellum samples represent gene expression values obtained from the GTEx consortium. Glioblastoma samples represent relative intensity measurements (Log₂) for each of the aforementioned genes obtained from GSE4412. In all cases, *n* indicates the number of samples used for statistical purposes. (c) Survival curves related to *TET3*, *RECK* and *WBP1L* gene expression. Kaplan–Meier plots represent the survival estimates of low or high gene expression groups for the previously stated genes. A median gene expression score was set as a criteria to stratify samples in the different categories. *p*-Value refers to differences in event rates between the Kaplan–Meier curves and was calculated with the Log-rank test function. Other basic statistics provided by the PROGgeneV2 tool, such as the hazard ratio (HR) and the confidence intervals are also provided for interpretation purposes.

TET3 levels are correlated with better prognosis of GBM patients

Next, we decided to validate the significance of our previous observations using a compendium of publicly available gene expression datasets.^{39–41} We observed a reduction of *RECK* expression levels in cancer brain samples as compared to glial cells from cortex or from white matter, while the levels of *WBP1L* were more variable between normal and tumoral tissues (Fig. 6a). On the other hand, *TET3* expression was highly correlated with *RECK* levels in human cerebellum and brain cortex (rob.cor 0.419 and 0.603, *p* <<< 0.001 in both tissues), but displayed no

or a negative correlation with *WBP1L* in the set of samples from the Genotype-Tissue Expression (GTEx) project (Fig. 6b, rob.cor –0.011 and 0.085 for cerebellum and brain cortex, respectively). Interestingly, although the tendency of these correlations was maintained to a slight extent in glioblastoma samples (Fig. 6b, data obtained from GSE4412), the positive correlation between *TET3* and *RECK* levels was weaker and not significant, probably due to tumor heterogeneity or the reduced expression of these candidate genes (Fig. 6b, rob.cor 0.216, *p* = 0.0613).

Finally, we observed an increased survival probability for GBM patients with high *TET3* or *RECK* expression levels

(Fig. 6c, data obtained from GSE4412). While *RECK* results were clearly above the significant threshold, and the survival differences between high and low *TET3* expression groups were at the margins of statistical significance, levels of *WBP1L* did not seem to have a significant impact on the survival of these GBM patients (Fig. 6c). This data indicates the potential importance of *TET3* and its direct downstream target genes in the etiology and prognosis of glioblastoma.

Discussion

Recent work has revealed the important role of 5hmC and TET proteins in the regulation of gene expression, including their potential impact on the epigenetic, the transcriptional and the alternative splicing landscape of mouse and human cells.^{42,43} While enhanced levels of 5hmC have been widely found in embryonic stem cells, as well as brain and neural related tissues,^{8–10} a notable reduction in 5hmC levels has been observed in multiple cancers,^{11–14,18} suggesting that some of the molecular networks governed by this epigenetic mark might be impaired during the tumorigenic process. Although mutations in IDH and TET proteins have emerged as potential candidates for the global loss of 5hmC,^{11,18} a significant subset of tumors might occur without any apparent genetic alterations in these family members. In this vein, recent work has demonstrated that oxygen gradients could play an important role in TET3 activity, at least in the context of embryonic stem cells.⁴⁴ This observation might also imply that oxygen deprivation in the tumor microenvironment could trigger the drastic deregulation of 5mC/5hmC levels by means of mechanisms other than mutations in *TET* or *IDH* genes. Therefore, in our study, we focused on the potential epigenetic alterations that mediate TET3 downregulation and a genome-wide reduction of 5hmC levels in brain tumors.

Interestingly, we found an increase of 5mC levels and a substantial reduction of 5hmC levels, as well as the global epigenetic downregulation of activating histone marks throughout the *TET3* gene, which correlated with a decrease in expression of *TET3* in glioma samples. Moreover, to confirm the relationships between the epigenetic alterations analyzed and *TET3* downregulation, we pharmacologically restored 5mC/5hmC and histone acetylation levels with Vitamin C treatment, which is known to stimulate TET protein activity,²⁰ as well as to restrain leukemia progression,⁴⁵ and in addition treated glioblastoma cells with SAHA, an inhibitor of the histone deacetylases HDAC1 and HDAC2.³⁶ While these pharmacological treatments are not specific for the activation of a given TET protein or the acetylation of a particular histone mark, intriguingly both approaches enhanced *TET3* expression, emphasizing the fundamental importance of these epigenetic modifications in gene regulation. Indeed, our data is further supported by recent studies which have shown the relevance of the aforementioned epigenetic marks. On the one hand, 5-hydroxymethylation of gene bodies and gene enhancers positively regulates gene expression of particular genes.⁴⁶ On the other, the parallel enhancement of

histone activating marks, such as H3K4me3, H3K9ac or H4K16ac, which has been positively correlated with gene activation,^{28,47,48} might reinforce the transcriptional activity of a given gene and maintain the robustness of the gene expression networks that are established in healthy conditions. We observed that restoration of *TET3* levels in the glioblastoma cell line LN229 markedly impaired the proliferative capacity of these cells. Interestingly, the growth defects observed in *TET3* overexpressing cells were not strongly related to programmed cell death under our experimental conditions but did point toward other cellular processes related to cell differentiation (see below). On the other hand, restoration of *TET3* levels partially recapitulated the levels of 5hmC found in human brain.^{25,26} Yet, in our analyses, the genome-wide association of 5hmC with other chromatin signatures reflected some discrepancies as compared to brain and glioma samples. We found a significant enrichment of 5hmC in genomic regions marked with H3K4me1 in both brain and *TET3* over-expressing glioblastoma cells. However, 5hmC mediated by *TET3* overexpression in LN229 cells was substantially enriched at Polycomb-repressed regions, bivalent enhancers and actively expressed genes, suggesting an overall redistribution of this epigenetic mark under our cell culture conditions. These subtle incongruences might be related to the use of immortal cell lines rather than related tissue counterparts,⁴⁹ as the initial chromatin status of glioblastoma cell lines might not fully recapitulate the epigenomic landscape of brain samples. Furthermore, overexpression of other TET3 interacting partners, such as the REST transcriptional complex, or the restoration of other TET family members, including *TET1* or *TET2* genes, might be required for the orchestrated regulation of 5hmC deposition observed in healthy brain tissue.⁴³

While recognizing the limitations of our experiments, we hypothesize that the impairment in tumor cell proliferation observed both *in vitro* and *in vivo* might well be caused by common rather than to different mechanisms in LN229 cells and in glioma samples. Indeed, GO analyses of genes decorated with 5hmC in brain and *TET3* transfected cells provided interesting cues to axogenesis and axon development, suggesting a potential role of 5hmC in neural differentiation. Although the role of TET proteins in neural differentiation has been well studied,^{23,50} recent work has demonstrated that other cell types, such as fibroblast, can be converted to neuron-like cells by *TET3* overexpression,³⁷ indicating that the molecular changes mediated by *TET3*, and possibly 5hmC, might act as driving forces to induce trans-differentiation toward neural lineages. Interestingly, upon restoration of *TET3* levels, we found increased expression of neural stem cell markers, such as SOX2, as well as other markers associated with the development of peripheral neurons, but not of oligodendrocytes or Schwann cells, indicating that the isolated activity of a given TET protein might be responsible for the establishment of defined transcriptional programs. However, we cannot rule out that the combined action of other TET members might be

required in order to achieve full differentiation potential. Nonetheless, the dedifferentiation pattern observed in cancer samples might be directly connected, at least in part, with the loss of TET protein activity and 5hmC in tumor cells.

In our study, we also identified downstream target genes whose expression might be affected by impairment in *TET3* expression and low 5hmC levels. Among them, *RECK*, an extracellular membrane-anchored protein with protease-inhibitor like domains which has been related to suppression of metastasis in glioma samples and other types of cancer,^{51,52} seems a plausible candidate for the reduced invasiveness of *TET3* expressing tumors. In this regard, it is important to mention that impairments in the expression of *RECK* isoforms, some of them with antagonistic capacities, have recently been described as potential modulators of the proliferative /migration capacity of such tumor cells.⁵³ As 5hmC tends to be associated with gene bodies and exons, it would be interesting to determine the impact of this epigenetic mark on the modulation of other transcripts which expression could be altered in 5hmC enriched tissues and their corresponding tumorigenic counterparts, such as in the case of normal brain and glioma conditions.

Our survival analyses allowed us to identify a significant association between high *TET3* and *RECK* expression levels and better overall survival of GBM patients. Along the same lines, high 5hmC levels have recently been reported to correlate with better prognosis of GBM patients.²⁶ Thus, altered 5hmC regulation mediated by *TET3*, or the combined activity of *TET3* and other *TET* family members, supports the notion that the presence of high 5hmC levels constitutes a favorable prognosis marker for the classification of GBM patients.²² To conclude, our work provides a detailed map of the *TET3*-mediated 5hmC changes that occur in glioma samples, which

may help to decipher the molecular mechanisms that are disrupted in brain tumors.

Acknowledgements

We sincerely apologize to all colleagues whose work could not be cited because of space constraints. We would like to thank Ronnie Lendum for editorial assistance, Cristina Martin (ISPA) and the Technical Services of University of Oviedo for professional support and all the members of the Cancer Epigenetics Lab (FINBA, IUOPA) for their positive feedback and helpful discussions. This work has been financially supported by the Plan Nacional de I+D+I 2013-2016/FEDER (PI15/00892 to M.F.F. and A.F.F.), the ISCIII-Subdirección General de Evaluación y Fomento de la Investigación (Miguel Servet contract CP11/00131 to A.F.F.); the Asturias Regional Government (GRUPIN14-052 to M.F.F.); FICYT (A.C. and M.G.); the Ministry of Economy and Competitiveness of Spain (J.R.T., Juan de la Cierva fellowship FJCI-2015-26965, V.L., Juan de la Cierva fellowship IJCI-2015-23316); Fundación Científica de la AECC (to R.G.U.); FINBA-ISPA (R.F.P.); IUOPA (G.F.B. and C.M.) and Fundación Ramón Areces (M.F.F.). A.F.F. is also financially supported by the Ministry of Economy and Competitiveness of Spain, the European Regional Development Fund (FEDER) and the Programa Retos de la Sociedad (RTC-2015-3393-1). The IUOPA is supported by the Obra Social Cajastur-Liberbank, Spain.

Author contributions

Study supervision, conception and design: Fernández AF, Fraga MF. Development of methodology: Carella A, García M, Tejedor JR, Urdinguio RG, Bayón GF, Mangas C. Acquisition of data: Carella A, García M, Urdinguio RG, Mangas C, Santamarina-Ojeda P, Pérez RF, Bigot TB, Sierra M, López V, García-Toraño E, Corte-Torres MD, Sáenz-de-Santa-María I, Mollejo M, Meléndez B, Astudillo A, Fernández AF, Fraga MF. Analysis and interpretation of data: Carella A, Tejedor JR, Bayón GF. Writing, review and/or revision of the manuscript: Carella A, Tejedor JR, Urdinguio RG, Bayón GF, Chiara MD, Fernández AF, Fraga MF.

References

1. Suzuki MM, Bird A. DNA methylation landscapes: provocative insights from epigenomics. *Nat Rev Genet* 2008;9:465–76.
2. Smith ZD, Meissner A. DNA methylation: roles in mammalian development. *Nat Rev Genet* 2013;14:204–20.
3. Jones PA. Functions of DNA methylation: islands, start sites, gene bodies and beyond. *Nat Rev Genet* 2012;13:484–92.
4. Shen H, Laird PW. Interplay between the cancer genome and epigenome. *Cell* 2013;153:38–55.
5. Tahiliani M, Koh KP, Shen Y, et al. Conversion of 5-methylcytosine to 5-hydroxymethylcytosine in mammalian DNA by MLL partner TET1. *Science* 2009;324:930–5.
6. Tan L, Shi YG. Tet family proteins and 5-hydroxymethylcytosine in development and disease. *Development* 2012;139:1895–902.
7. Bocker MT, Tuorto F, Raddatz G, et al. Hydroxylation of 5-methylcytosine by TET2 maintains the active state of the mammalian HOXA cluster. *Nat Commun* 2012;3:818.
8. Wossidlo M, Nakamura T, Lepikhov K, et al. 5-Hydroxymethylcytosine in the mammalian zygote is linked with epigenetic reprogramming. *Nat Commun* 2011;2:241.
9. Szulwach KE, Li X, Li Y, et al. 5-hmC-mediated epigenetic dynamics during postnatal neurodevelopment and aging. *Nat Neurosci* 2011;14:1607–16.
10. Kriaucionis S, Heintz N. The nuclear DNA base 5-hydroxymethylcytosine is present in Purkinje neurons and the brain. *Science* 2009;324:929–30.
11. Lian CG, Xu Y, Ceol C, et al. Loss of 5-hydroxymethylcytosine is an epigenetic hallmark of melanoma. *Cell* 2012;150:1135–46.
12. Haffner MC, Chaux A, Meeker AK, et al. Global 5-hydroxymethylcytosine content is significantly reduced in tissue stem/progenitor cell compartments and in human cancers. *Oncotarget* 2011;2:627–37.
13. Kraus TFJ, Kolck G, Greiner A, et al. Loss of 5-hydroxymethylcytosine and intratumoral heterogeneity as an epigenomic hallmark of glioblastoma. *Tumour Biol* 2015;36:8439–46.
14. Thomson JP, Ottaviano R, Unterberger EB, et al. Loss of Tet1-associated 5-hydroxymethylcytosine is concomitant with aberrant promoter hypermethylation in liver cancer. *Cancer Res* 2016;76:3097–108.
15. Turcan S, Rohr D, Goenka A, et al. IDH1 mutation is sufficient to establish the glioma hypermethylator phenotype. *Nature* 2012;483:479–83.
16. Scourcier L, Mouly E, Bernard OA. TET proteins and the control of cytosine demethylation in cancer. *Genome Med* 2015;7:9.
17. Xu W, Yang H, Liu Y, et al. Oncometabolite 2-hydroxyglutarate is a competitive inhibitor of α-ketoglutarate-dependent dioxygenases. *Cancer Cell* 2011;19:17–30.
18. Yang H, Liu Y, Bai F, et al. Tumor development is associated with decrease of TET gene expression and 5-methylcytosine hydroxylation. *Oncogene* 2013;32:663–9.
19. Bachman M, Uribe-Lewis S, Yang X, et al. 5-Hydroxymethylcytosine is a predominantly stable DNA modification. *Nat Chem* 2014;6:1049–55.
20. Hore TA, von Meyenn F, Ravichandran M, et al. Retinol and ascorbate drive erasure of epigenetic memory and enhance reprogramming to naïve pluripotency by complementary mechanisms. *Proc Natl Acad Sci USA* 2016;113:12202–7.

21. Jin S-G, Jiang Y, Qiu R, et al. 5-Hydroxymethylcytosine is strongly depleted in human cancers but its levels do not correlate with IDH1 mutations. *Cancer Res* 2011;71:7360–5.
22. Orr BA, Haffner MC, Nelson WG, et al. Decreased 5-hydroxymethylcytosine is associated with neural progenitor phenotype in normal brain and shorter survival in malignant glioma. *PLoS One* 2012;7:e41036.
23. Li T, Yang D, Li J, et al. Critical role of Tet3 in neural progenitor cell maintenance and terminal differentiation. *Mol Neurobiol* 2015;51:142–54.
24. Cui Q, Yang S, Ye P, et al. Downregulation of TLX induces TET3 expression and inhibits glioblastoma stem cell self-renewal and tumorigenesis. *Nat Commun* 2016;7:10637.
25. Fernandez AF, Bayón GF, Sierra MI, et al. Loss of ShmC identifies a new type of aberrant DNA hypermethylation in glioma. *Hum Mol Genet* 2018;27:3046–59.
26. Johnson KC, Houseman EA, King JE, et al. 5-Hydroxymethylcytosine localizes to enhancer elements and is associated with survival in glioblastoma patients. *Nat Commun* 2016;7:13177.
27. Raiber E-A, Bernaldi D, Martínez Cuesta S, et al. Base resolution maps reveal the importance of 5-hydroxymethylcytosine in a human glioblastoma. *NPJ Genom Med* 2017;2:6.
28. Taylor GCA, Eskeland R, Hekimoglu-Balkan B, et al. H4K16 acetylation marks active genes and enhancers of embryonic stem cells but does not alter chromatin compaction. *Genome Res* 2013;23:2053–65.
29. Fraga MF, Ballestar E, Villar-Garea A, et al. Loss of acetylation at Lys16 and trimethylation at Lys20 of histone H4 is a common hallmark of human cancer. *Nat Genet* 2005;37:391–400.
30. Roadmap Epigenomics Consortium, Kundaje A, Meuleman W, et al. Integrative analysis of 111 reference human epigenomes. *Nature* 2015;518:317–30.
31. Chen X, Zhang M, Gan H, et al. A novel enhancer regulates MGMT expression and promotes temozolomide resistance in glioblastoma. *Nat Commun* 2018;9:2949.
32. Sim FJ, Windrem MS, Goldman SA. Fate determination of adult human glial progenitor cells. *Neuron Glia Biol* 2009;5:45–55.
33. Grzmil M, Morin P, Lino MM, et al. MAP kinase-interacting kinase 1 regulates SMAD2-dependent TGF-β signaling pathway in human glioblastoma. *Cancer Res* 2011;71:2392–402.
34. Günther HS, Schmidt NO, Phillips HS, et al. Glioblastoma-derived stem cell-enriched cultures form distinct subgroups according to molecular and phenotypic criteria. *Oncogene* 2008;27:2897–909.
35. Xu X, Stoyanova EI, Lemiesz AE, et al. Species and cell-type properties of classically defined human and rodent neurons and glia. *Elife* 2018;7:e37551.
36. Dudakovic A, Evans JM, Li Y, et al. Histone deacetylase inhibition promotes osteoblast maturation by altering the histone H4 epigenome and reduces Akt phosphorylation. *J Biol Chem* 2013;288:28783–91.
37. Zhang J, Chen S, Zhang D, et al. Tet3-mediated DNA demethylation contributes to the direct conversion of fibroblast to functional neuron. *Cell Rep* 2016;17:2326–39.
38. ENCODE Project Consortium. An integrated encyclopedia of DNA elements in the human genome. *Nature* 2012;489:57–74.
39. Auvergne RM, Sim FJ, Wang S, et al. Transcriptional differences between normal and glioma-derived glial progenitor cells identify a core set of dysregulated genes. *Cell Rep* 2013;3:2127–41.
40. GTEx Consortium. Human genomics. The genotype-tissue expression (GTEx) pilot analysis: multitissue gene regulation in humans. *Science* 2015;348:648–60.
41. Freije WA, Castro-Vargas FE, Fang Z, et al. Gene expression profiling of gliomas strongly predicts survival. *Cancer Res* 2004;64:6503–10.
42. Pastor WA, Pape UJ, Huang Y, et al. Genome-wide mapping of 5-hydroxymethylcytosine in embryonic stem cells. *Nature* 2011;473:394–7.
43. Perera A, Eisen D, Wagner M, et al. TET3 is recruited by REST for context-specific hydroxymethylation and induction of gene expression. *Cell Rep* 2015;11:283–94.
44. Burr S, Caldwell A, Chong M, et al. Oxygen gradients can determine epigenetic asymmetry and cellular differentiation via differential regulation of Tet activity in embryonic stem cells. *Nucleic Acids Res* 2018;46:1210–26.
45. Cimmino L, Dolgalev I, Wang Y, et al. Restoration of TET2 function blocks aberrant self-renewal and leukemia progression. *Cell* 2017;170:1079–1095.e20.
46. Jin S-G, Wu X, Li AX, et al. Genomic mapping of 5-hydroxymethylcytosine in the human brain. *Nucleic Acids Res* 2011;39:5015–24.
47. Liang G, Lin JCY, Wei V, et al. Distinct localization of histone H3 acetylation and H3-K4 methylation to the transcription start sites in the human genome. *Proc Natl Acad Sci USA* 2004;101:7357–62.
48. Kouzarides T. Chromatin modifications and their function. *Cell* 2007;128:693–705.
49. Goodspeed A, Heiser LM, Gray JW, et al. Tumor-derived cell lines as molecular models of cancer pharmacogenomics. *Mol Cancer Res* 2016;14:3–13.
50. Li X, Yao B, Chen L, et al. Ten-eleven translocation 2 interacts with forkhead box O3 and regulates adult neurogenesis. *Nat Commun* 2017;8:15903.
51. Clark JCM, Thomas DM, Choong PFM, et al. RECK--a newly discovered inhibitor of metastasis with prognostic significance in multiple forms of cancer. *Cancer Metastasis Rev* 2007;26:675–83.
52. Silveira Corrêa TC, Massaro RR, Brohem CA, et al. RECK-mediated inhibition of glioma migration and invasion. *J Cell Biochem* 2010;110:52–61.
53. Trombetta-Lima M, Winnischhofer SMB, Demasi MAA, et al. Isolation and characterization of novel RECK tumor suppressor gene splice variants. *Oncotarget* 2015;6:33120–33.